



## Research paper

## Effects of Ta-oxide interlayer on the Schottky barrier parameters of Ni/n-type Ge Schottky barrier diode



Hoon-Ki Lee <sup>a</sup>, I. Jyothi <sup>a</sup>, V. Janardhanam <sup>a</sup>, Kyu-Hwan Shim <sup>a</sup>, Hyung-Joong Yun <sup>a,b</sup>, Sung-Nam Lee <sup>c</sup>, Hyobong Hong <sup>d</sup>, Jae-Chan Jeong <sup>d</sup>, Chel-Jong Choi <sup>a,\*</sup>

<sup>a</sup> School of Semiconductor and Chemical Engineering, Semiconductor Physics Research Center, Chonbuk National University, Jeonju 561-756, Republic of Korea

<sup>b</sup> Division of Material Science, Korea Basic Science Institute, Daejeon 305-806, Republic of Korea

<sup>c</sup> Department of Nano-Optical Engineering, Korea Polytechnic University, Siheung 429-793, Republic of Korea

<sup>d</sup> Electronics & Telecommunication Research Institute (ETRI), Daejeon 305-700, Republic of Korea

## ARTICLE INFO

## Article history:

Received 12 January 2016

Received in revised form 10 May 2016

Accepted 4 June 2016

Available online 06 June 2016

## Keywords:

Schottky barrier diode

Ta-oxide

Interface states

Ge

Ni

Current conduction

## ABSTRACT

The effect of Ta-oxide interlayer on the Schottky barrier parameters of Ni/n-type Ge Schottky barrier diode (SBD) was investigated. The introduction of the Ta-oxide interlayer in-between Ni film and Ge substrate resulted in an increase in the barrier height as against the conventional Ni/n-type Ge SBD. Furthermore, increase in the thickness of the Ta-oxide interlayer led to the increase in barrier height and decrease in ideality factor, which could be associated with the improvement of interface quality of Schottky junction. 5 nm-thick Ta-oxide interlayer was more stoichiometric than 3 nm-thick Ta-oxide one, which was effective in the reduction of interface state density and ideality factor. An investigation of the electric field dependence of the reverse current in the Ni/n-type Ge SBDs with and without Ta-oxide revealed that the Poole-Frenkel emission mechanism dominates the current conduction of both devices in the reverse bias region.

© 2016 Elsevier B.V. All rights reserved.

## 1. Introduction

Germanium (Ge) is a promising candidate as a channel material of future complementary metal-oxide semiconductor (CMOS) due to its inherent property of high carrier mobility of both electrons and holes than Si, which is suitable for the enhancement of device performance [1]. In order to realize high performance Ge-based devices, well controlled electrical contacts are essential. Metal-semiconductor (MS) Schottky contacts are basic device structure in semiconductor technology and have been widely used in semiconductor industry [2]. Due to the technological importance of the Schottky contacts, there have been considerable efforts to fully understand their electrical properties over the past several decades [3]. In general, the interface property of Schottky junction is one of the most important key factors to determine the operation and performance of Schottky devices. Practically, the metal-semiconductor contact is not intimate contacts but it possesses a thin insulating interfacial layer between metal and semiconductor, unless it specially fabricated [4]. The existence of such an interfacial layer converts the MS Schottky device into a metal-insulator-semiconductor (MIS) Schottky device, which gives a significant effect on its Schottky barrier parameters such as barrier height, ideality factor, interface trap

density, and series resistance [5,6]. In a recent year, MIS Schottky barrier diodes (SBDs) become more and more important in a great variety of fields of modern semiconductor technology since the thin insulator layer facilitates the modification of Schottky barrier properties [3,7,8]. Until now, there are a vast number of experimental and theoretical studies on electrical characteristics of MIS SBDs [9,10]. They showed that the operation and reliability of MIS SBDs are strongly dependent on the quality and the technological controllability of the thin insulator layer between metal and semiconductor. In particular, MIS structures are preferred to Ge-based Schottky devices since insulator layer allows a modification of the effective barrier height caused by affecting interfacial potential barrier of Schottky junction [11,12]. In other word, by employing thin insulator layer, Schottky barrier properties of Ge-based Schottky devices can be effectively improved. Despite prominent features of MIS structures, however, the detail knowledge about MIS-type Ge Schottky devices remains unclear. Moreover, there are only a few studies focused on the modulation of the electrical characteristics of Ge-based Schottky devices with variable thickness of the insulating layer [13,14]. In this work, we fabricated Ni/n-type Ge SBDs with 3 and 5 nm-thick Ta-oxide interlayer and investigated their electrical properties using the current-voltage (*I*-*V*) characteristics. Emphasis is placed on investigating the effect of the thickness of Ta-oxide interlayer on Schottky barrier properties of Ni/n-type Ge SBD. It will be shown that the introduction of Ta-oxide interlayer in-between Ni film and Ge

\* Corresponding author.

E-mail address: [cjchoi@jbnu.ac.kr](mailto:cjchoi@jbnu.ac.kr) (C.-J. Choi).

substrate is effective for the increase in barrier height and a decrease in the interface states. Furthermore, the possible current conduction mechanism of the Schottky contacts modified using Ta-oxide interlayer in the reverse bias will be also examined.

## 2. Experimental details

Sb-doped n-type Ge (100) wafers with a carrier concentration of  $1 \times 10^{18} \text{ cm}^{-3}$  were used as a starting material in this work. The wafers were initially cleaned in an ultrasonic bath of acetone and isopropanol for 5 min in each for the removal of contaminants, followed by the removal of the native oxide using buffered oxide etch (BOE) solution. The square patterns with a dimension of  $300 \mu\text{m} \times 300 \mu\text{m}$  were defined by means of standard photolithography. Afterward, the patterned wafers were dipped into a BOE solution, and immediately loaded into the E-beam evaporation chamber. The 3- or 5-nm thick Ta-oxide film and 50-nm thick Ni film were sequentially deposited by the E-beam evaporation under a pressure of  $1 \times 10^{-6}$  Torr, followed by patterning using lift-off process. Transmission electron microscope (TEM) measurements (not shown here) revealed that the deposited Ta-oxide films had an amorphous nature. Finally, Al metallization was made on the back side of the Ge substrate as Ohmic contact. For a comparison, the Ni Schottky contact without a Ta-oxide interlayer was fabricated on n-type Ge wafer under the same process conditions. The  $I$ - $V$  characteristics of the Ni/n-type Ge Schottky diode with and without Ta-oxide interlayer were measured using a semiconductor parameter analyzer (Agilent4155A). X-ray photoemission spectroscopy (XPS; K-alpha, Thermo scientific Inc.) was employed to identify chemical bonding nature of Ta-oxide film. The C1 s peak in the air was fixed to 285.0 eV to set the binding energy scale and the XPS data processing (deconvolution) was performed using CASAXPS software (Version 2.3.16., U.K.).

## 3. Results and discussion

Fig. 1 shows the room temperature  $I$ - $V$  characteristics of the Ni/n-type Ge SBDs with and without the Ta-oxide interlayer. All the devices exhibited relatively good rectifying behavior. The introduction of Ta-oxide interlayer led to the decrease in reverse leakage current. Moreover, reverse leakage current decreased with increasing the thickness of Ta-oxide interlayer. This implies the modulation of Schottky barrier height of Ni/n-type Ge Schottky contact caused by presence of Ta-oxide interlayer. Based on the thermionic emission theory, the Schottky barrier parameters of Ni/n-type Ge SBDs with and without the Ta-oxide interlayer were quantitatively evaluated. When a Schottky contact with

series resistance and an interfacial layer is considered with respect to forward bias voltages of  $V > 3kT/q$ , we assumed that the net current is due to thermionic emission current that can be described as [9]:

$$I = I_0 \exp \left[ \frac{q(V - IR_s)}{nkT} \right] \left\{ 1 - \exp \left[ \frac{q(V - IR_s)}{kT} \right] \right\} \quad (1)$$

where  $I$  is the measured current,  $V$  is the applied voltage across the junction,  $R_s$  is the series resistance,  $q$  is the electronic charge,  $k$  is the Boltzmann's constant,  $T$  is the absolute temperature is kelvin,  $n$  is the ideality factor, and  $I_0$  is the saturation current derived from the straight line intercept of the plot of  $\ln(I)$  versus  $V$  at  $V = 0$  given by

$$I_0 = AA^* T^2 \exp \left( \frac{q\Phi_{b0}}{kT} \right) \quad (2)$$

where  $A$  is the device area,  $A^*$  is the Richardson constant ( $140 \text{ A cm}^{-2} \text{ K}^{-2}$  for n-type Ge was assumed in this study),  $\Phi_{b0}$  is the barrier height determined from  $I_0$  using

$$\Phi_{b0} = \frac{kT}{q} \ln \left( \frac{AA^* T^2}{I_0} \right). \quad (3)$$

The ideality factor  $n$  was determined from the slope of the linear region of the forward bias  $\ln(I)$ - $V$  plot, and measures the conformity of the diode due to pure thermionic emission, which can be expressed by

$$n = \frac{q}{kT} \left( \frac{dV}{d(\ln I)} \right). \quad (4)$$

The values of barrier height and ideality factor extracted using the forward bias  $\ln(I)$ - $V$  plot were summarized in Table 1. It is clear that the ideality factor and barrier height were strongly affected by the presence of Ta-oxide interlayer. The barrier height and ideality factor for the Ni/n-type Ge SBD were obtained as 0.46 eV and 1.57, respectively. The barrier height of the Ni/n-type Ge SBD was lower than those reported previously [15,16], associated with the high doping concentration of the Ge substrate used in this work. On the other hand, the barrier height and ideality factor of the Ni/n-type Ge Schottky SBD with 3 nm-thick Ta-oxide interlayer were 0.50 eV and 1.52, respectively and those of the SBD with 5 nm-thick Ta-oxide interlayer were 0.56 eV and 1.15, respectively. Namely, the barrier height of Ni/Ta-oxide/n-type Ge Schottky SBDs was higher than that of conventional Ni/n-type Ge Schottky SBD. This implies that Ta-oxide interlayer influenced the interfacial potential barrier of the Ni/n-type Ge Schottky junction, resulting in a modification of the effective barrier height. Furthermore, barrier height increased with increasing the thickness of Ta-oxide interlayer as reflected in the decrease in reverse leakage current. Such an increase in barrier height could be attributed to the amendment of the interface states that control the barrier height, which will be discussed later. For all devices, the ideality factors were greater than unity, implying their deviation from the ideal thermionic emission. This could be due to the potential drop in the interface layer, the presence of excess current and the recombination current through the interfacial states between the semiconductor and interlayer [17]. Also, the possible reasons include various effects such as in homogeneities of the interlayer, series

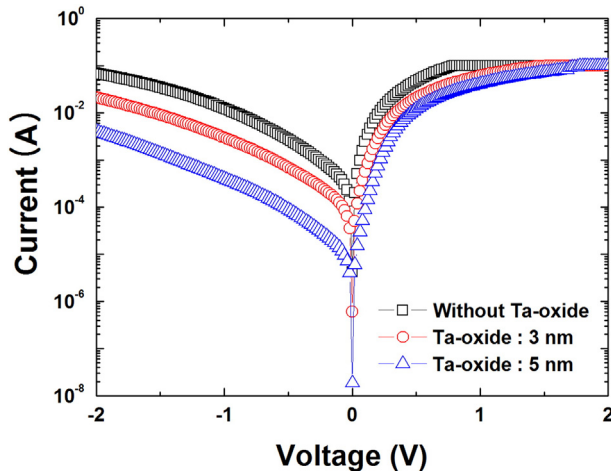


Fig. 1.  $I$ - $V$  characteristics of the Ni/n-type Ge SBDs with and without the Ta-oxide interlayer measured at room temperature.

Table 1

Schottky barrier parameters measured using various methods (barrier height, ideality factor, and series resistance) of Ni/n-type Ge SBDs with and without Ta-oxide interlayer.

Sample	Barrier height (eV)			Ideality factor (n)		Series resistance ( $\Omega$ )	
	$I$ - $V$	$H(I)$	Norde	$I$ - $V$	$dV/d(\ln I)$	$H(I)$	$dV/d(\ln I)$
Without Ta-oxide	0.46	0.48	0.47	1.57	3.25	4.1	4.5
Ta-oxide: 3 nm	0.50	0.64	0.52	1.52	2.48	9.8	11.1
Ta-oxide: 5 nm	0.56	0.65	0.60	1.15	2.35	15.3	14.9

resistance, non-uniform distribution of the interfacial charges, specific interface structure and the fabrication-induced defects at the interface [18]. Similarly, Tung [19] reported that higher values of ideality factor could be associated with the presence of a wide distribution of low Schottky barrier height patches caused by a laterally inhomogeneous barrier height.

Generally, the forward bias  $I$ - $V$  characteristics are linear on a semi-logarithmic scale in the low forward bias region. However, due to the effect of series resistance, they deviate considerably from linearity at higher voltages. Namely, the evaluation of series resistance is essential to understanding fully the electrical properties of Ni/n-type Ge SBDs with and without Ta-oxide interlayer. In general, the series resistance along with other Schottky barrier parameters such as the barrier height and ideality factor can be evaluated using Cheung's method [20]. Cheung's function can be expressed as

$$\frac{dV}{d(\ln I)} = \frac{nkT}{q} + IR_S \quad (5)$$

$$H(I) = V - n \left( \frac{kT}{q} \right) \ln \left( \frac{I}{AA^{**}T} \right) = n\phi_{b0} + IR_S. \quad (6)$$

Fig. 2(a) shows the plot of  $dV/d(\ln I)$  versus  $I$  for the Ni/n-type Ge SBDs with and without Ta-oxide interlayer. A straight line for the data in the downward curvature region of the forward bias  $I$ - $V$  characteristics should be obtained following Eq.(5) and is evident in Fig. 2(a). The

slope and y-axis intercept of the  $dV/d(\ln I)$ - $I$  plot yields series resistance and ideality factor, respectively. From the linear fit of  $dV/d(\ln I)$ - $I$  plot, the series resistance and ideality factor Ni/n-type Ge SBD were calculated to be 4.5  $\Omega$  and 3.25, respectively. Whilst the series resistance and ideality factor of Ni/n-type Ge SBD with 3 nm-thick Ta-oxide interlayer were 11.1  $\Omega$  and 2.48, respectively and those of the SBD with 5 nm-thick Ta-oxide interlayer were 14.9  $\Omega$  and 2.35, respectively. It was observed that there existed a large difference between the values of ideality factor obtained from the forward bias  $\ln(I)$ - $V$  plot (Fig. 1) and the  $dV/d(\ln I)$ - $I$  plot (Fig. 2(a)). This could be associated with the series resistance caused by voltage drop across the interlayer. According to Eq. (6), the plot of  $H(I)$  versus  $I$  must be linear, as shown in Fig. 2(b). The slope and y-intercept of this plot yield series resistance barrier height by using the value of ideality factor determined from the  $dV/d(\ln I)$  versus  $I$  plot (Fig. 3(a)). From the  $H(I)$  versus  $I$  plot (Fig. 2(b)), the series resistance were obtained as 4.1, 9.8 and 15.3  $\Omega$  for the Ni/n-type Ge SBDs without and with 3 and 5 nm-thick Ta-oxide interlayer, respectively and corresponding barrier heights were extracted to be 0.48, 0.64 and 0.65 eV, respectively. The differences in the values of the barrier heights obtained from the forward bias  $\ln(I)$ - $V$  and Cheung's methods could be attributed to the extraction from different regions of the forward bias  $I$ - $V$  characteristics. In particular, the values of series resistance obtained from the  $dV/d(\ln I)$ - $I$  plot closely matched to those obtained from the  $H(I)$ - $V$  plot, implying the consistency of the Cheung's method.

Norde proposed an empirical function to calculate the barrier height for Schottky contact [21]. The Norde function is defined as

$$F(V) = \frac{V}{\gamma} - \frac{kT}{q} \ln \left( \frac{I(V)}{AA^{**}T^2} \right). \quad (7)$$

The barrier height is given by,

$$\phi_{b0} = F(V_{min}) + \frac{V_{min}}{\gamma} - \frac{kT}{q} \quad (8)$$

where  $F(V_{min})$  is the minimum value of  $F(V)$  and  $V_{min}$  is the equivalent voltage. Fig. 3 shows plot of  $F(V_{min})$  versus  $V$  for the Ni/n-type Ge SBDs with and without Ta-oxide interlayer. From Norde's method, the barrier height was extracted to be 0.47 eV for the Ni/n-type Ge SBD, while the values were obtained as 0.52, and 0.60 eV for Ni/n-type Ge SBDs with 3 and 5 nm-thick Ta-oxide interlayer, respectively. As shown in table I, there was a discrepancy in the values of the barrier heights obtained from the Norde method and other methods. Such a discrepancy could be related to the deviation of the present devices from ideal thermionic

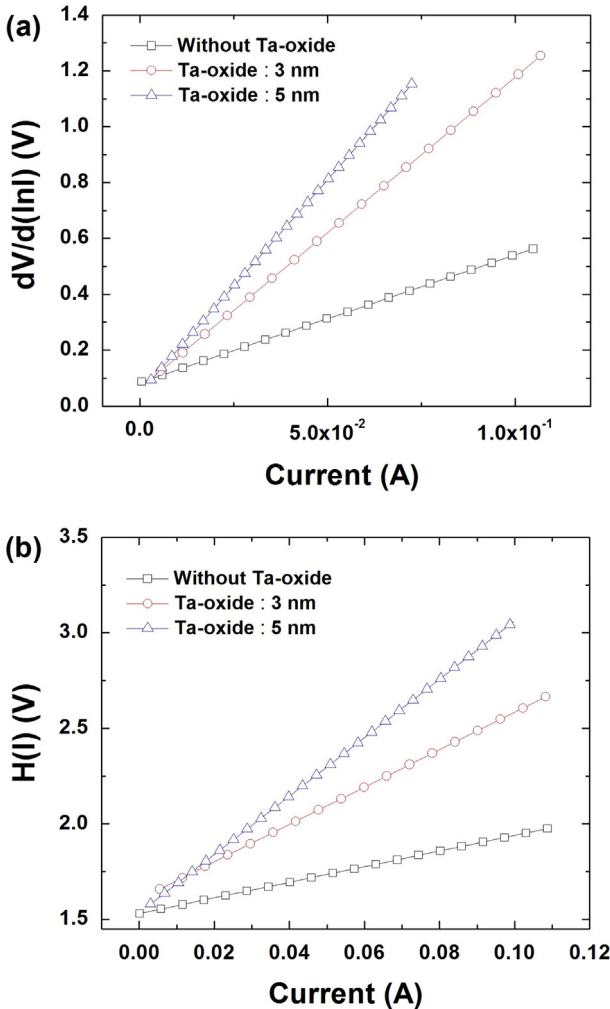


Fig. 2. (a)  $dV/d(\ln I)$ - $I$  and (b)  $H(I)$ - $I$  plots from the forward  $I$ - $V$  characteristics of Ni/n-type Ge SBDs with and without Ta-oxide interlayer.

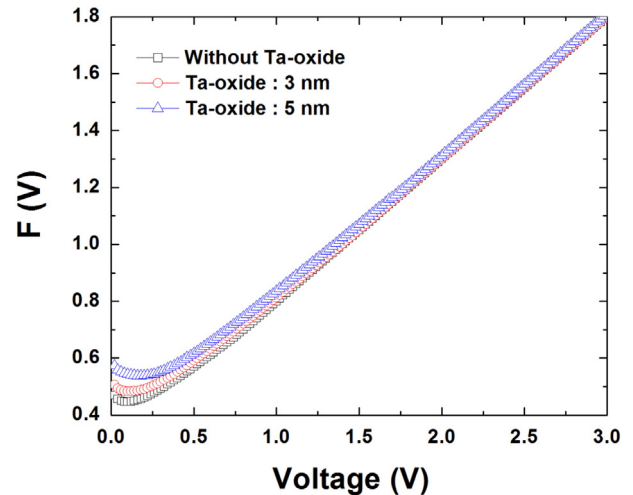


Fig. 3. Plot of  $F(V_{min})$  versus  $V$  for the Ni/n-type Ge SBDs with and without Ta-oxide interlayer.

emission [22]. Furthermore, the Norde's method may not be suitable for the rectifying junctions with high ideality factor, which are not compatible with the pure thermionic emission [23].

For SBDs having interface states in equilibrium with semiconductor, the ideality factor, becomes greater than unity, as proposed by Card and Rhoderick [24]. The energy density distribution of the interface states ( $N_{ss}$ ) can be calculated from the forward bias  $I$ - $V$  data by considering the voltage-dependent ideality factor  $n(V)$  and effective barrier height  $\Phi_e$ . The interface state density is given by:

$$N_{ss} = \frac{1}{q} \left\{ \frac{\varepsilon_i}{\delta} [n(V) - 1] - \frac{\varepsilon_s}{W_d} \right\} \quad (9)$$

where  $\varepsilon_i$  and  $\varepsilon_s$  are the permittivity of the insulator layer and semiconductor, respectively,  $\delta$  is the thickness of the interfacial layer,  $W_d$  is the width of the space-charge region, and  $n(V)$  is the voltage dependent ideality factor given by  $n(V) = V/(kT/q) \ln(I/I_0)$ . For n-type semiconductors, the energy of the interface states with respect to the bottom of the conduction band ( $E_C$ ) at the surface of the semiconductor is given by

$$E_C - E_{ss} = q\Phi_e - qV \quad (10)$$

where  $V$  is the voltage drop across the depletion layer and  $\Phi_e$  is the effective barrier height given by

$$\Phi_e = \Phi_b + \beta V \quad (11)$$

where  $\beta$  is the voltage coefficient of the effective barrier height, given by

$$\beta = \frac{d\Phi_e}{dV} = 1 - \frac{1}{n(V)}. \quad (12)$$

Fig. 4 shows the plot of  $N_{ss}$  versus  $E_C - E_{ss}$  taken from the Ni/n-type Ge SBDs with and without Ta-oxide interlayer. For all devices,  $N_{ss}$  increased exponentially from the mid gap towards the bottom of the conduction band. It should be noted that at any particular energy level, Ni/n-type Ge SBDs with Ta-oxide interlayer showed lower  $N_{ss}$  than Ni/n-type Ge SBD without Ta-oxide interlayer. Moreover, the  $N_{ss}$  of Ni/n-type Ge SBD with 5 nm-thick Ta-oxide interlayer was lower than that with 3 nm-thick Ta-oxide interlayer. This implies that the Ge surface was effectively passivated by thicker Ta-oxide interlayer, which would reduce the number of dangling bonds at the Ge surface, and therefore the  $N_{ss}$ .

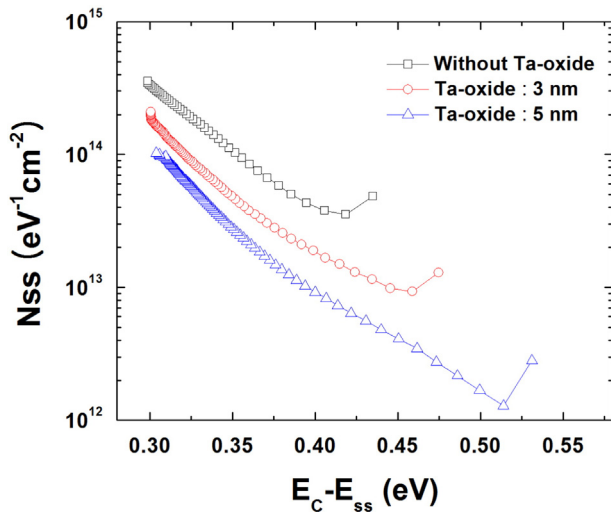


Fig. 4. Plot of  $N_{ss}$  versus  $E_C - E_{ss}$  taken from the Ni/n-type Ge SBDs with and without Ta-oxide interlayer.

Fig. 5 represents XPS spectra taken from the interface between Ta-oxide interlayer and Ge substrate of Ni/n-type Ge SBDs with 3 and 5 nm-thick Ta-oxide interlayer. The curve-fitting processing was employed to identify the composition and the chemical state throughout the film. In the peak fitting, binding energy separation and area ratio of Ta 4f7/2 and Ta 4f5/2 were kept constant at 1.9 eV and 1.3–1.4, respectively. Both samples showed Ge 3d and Ta 4f peaks, of which individual positions were almost identical. Two peaks at the binding energy of 23.7 and 21.8 eV were assigned to the metallic (Ta-Ta) components [25]. Features at 26.1 eV (Ta 4f 5/2) and 28.0 eV (Ta 4f 7/2) were identified as  $Ta^{5+}$  oxidation state corresponding to  $Ta_2O_5$ , which is most stable Ta-oxide [26]. The additional Ta-oxide peaks at lower binding energies of 25.6 eV and 27.5 eV with respect to the  $Ta^{5+}$  states were attributed to the  $Ta^{4+}$  oxide state [27]. Namely, XPS examination clearly revealed that Ta-oxide interlayer having inhomogeneous chemical states were formed during E-beam evaporation process. It should be noted that area ratio of  $Ta^{4+}$  to  $Ta^{5+}$  peaks ( $Ta^{4+}/Ta^{5+}$  ratio) of Ni/n-type Ge SBDs with 5 nm-thick Ta-oxide interlayer (0.59) was much lower than that with 3 nm-thick Ta-oxide interlayer (1.36). This implies that 5 nm-thick Ta-oxide interlayer had a higher amount of stoichiometric Ta-oxide (i.e.,  $Ta_2O_5$ ) than 3 nm-thick Ta-oxide interlayer. However, the corresponding high resolution TEM

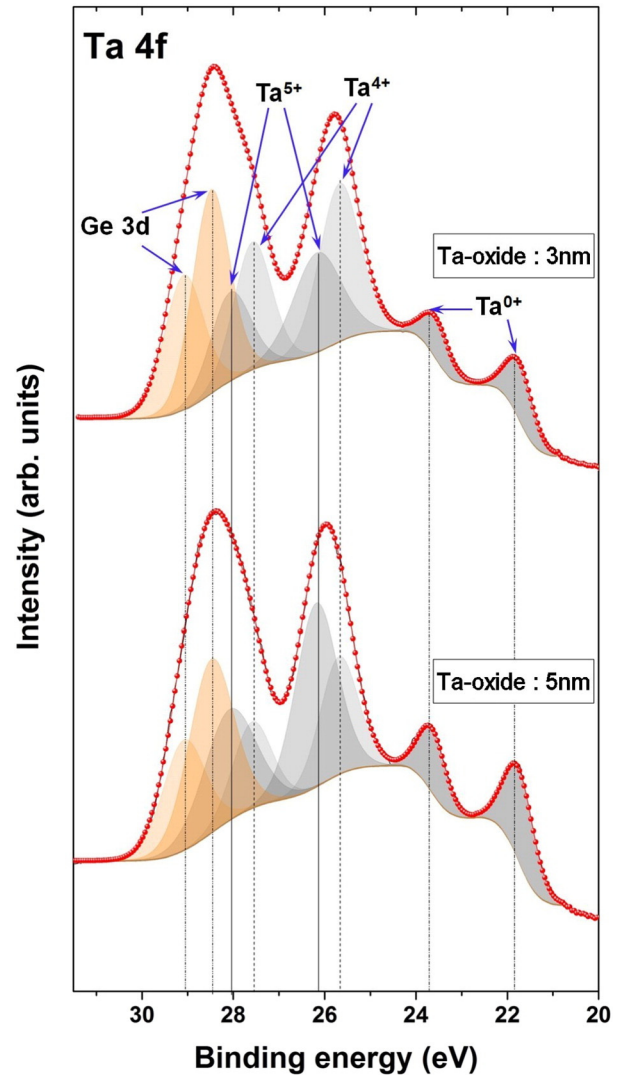


Fig. 5. XPS spectra taken from the interface between Ta-oxide interlayer and Ge substrate of Ni/n-type Ge SBDs with 3 and 5 nm-thick Ta-oxide interlayer.



measurements (not shown here) did not provide a direct evidence for 5 nm-thick Ta-oxide interlayer being more stoichiometric than Ta-oxide composition than 3 nm-thick Ta-oxide one, which could be associated with a low phase contrast in high resolution TEM image typical for amorphous materials. It is obvious that as compared to stoichiometric oxides, the non-stoichiometric oxides have more defects, which could be one of the major sources of interface states [28–30]. Thus, 5 nm-thick Ta-oxide interlayer having less defects than 3 nm-thick Ta-oxide one was effective in the improvement of interface quality, which could be responsible for lower interface states and ideality factor of Ni/n-type Ge SBDs with 5 nm-thick Ta-oxide interlayer.

From Fig. 1, it is clear that the reverse current of the Ni/n-type Ge SBDs with and without Ta-oxide interlayer increased with increasing bias but was not saturated. The carrier recombination in the depletion region and image force lowering of the barrier height often dominates the reverse leakage current since the reverse bias increases the electric field in the junction. The conduction mechanism dominating the reverse leakage current in the Ni/n-type Ge Schottky diode with and without Ta-oxide interlayer was investigated by considering Poole-Frenkel emission and Schottky emission mechanisms across the junction. The reverse current through the diode when dominated by the Poole-Frenkel emission mechanism is given by [31]

$$I_R \propto E \exp\left(\frac{1}{kT} \sqrt{\frac{qE}{\pi\epsilon}}\right) \quad (13)$$

and the contribution to reverse current when dominated by Schottky emission mechanism is given as [31]

$$I_R \propto T^2 \exp\left(\frac{1}{2kT} \sqrt{\frac{qE}{\pi\epsilon}}\right) \quad (14)$$

where  $E$  is the maximum electric field in the junction. The plots of Poole-Frenkel emission ( $I_R/E$  versus  $E^{1/2}$  plot) and Schottky emission ( $I_R/T^2$  versus  $E^{1/2}$  plot) for the Ni/n-type Ge SBDs without and with Ta-oxide interlayer are shown in Fig. 6. The plots produce linear curve whose slope can be expressed as [31]

$$S = \frac{q}{nkT} \sqrt{\frac{q}{\pi\epsilon}} \quad (15)$$

where  $n = 1$  for Poole-Frenkel emission and  $n = 2$  for Schottky emission. The ideal slopes for Poole-Frenkel emission and Schottky emission were calculated to be 0.0073 and  $0.0036(\text{V cm}^{-1})^{-1/2}$  at 300 K, respectively. For all devices, the plots of  $I_R/E$  versus  $E^{1/2}$  (Fig. 6(a)) and  $I_R/T^2$  versus  $E^{1/2}$  (Fig. 6(b)) were linear with positive slopes. The slopes obtained from fit to the plots of  $I_R/E$  versus  $E^{1/2}$  and  $I_R/T^2$  versus  $E^{1/2}$  varied in the range of 0.00602–0.00671  $(\text{V cm}^{-1})^{-1/2}$  and 0.00728–0.00796  $(\text{V cm}^{-1})^{-1/2}$ , respectively. Namely, irrespective of the presence of Ta-oxide interlayer, the slopes determined from the data fit were closer to the theoretical value of Poole-Frenkel emission than that of Schottky emission. Hence, the Poole-Frenkel emission mechanism was believed to be the dominant current transport mechanism governing the reverse leakage current of Ni/n-type Ge SBDs without and with Ta-oxide interlayer. In this mechanism, the carrier transport occurs from the metal into conductive defects via trap states rather than by direct emission from the metal.

#### 4. Conclusion

We investigate the effect of Ta-oxide interlayer on the electrical characteristics of the Ni/n-type Ge SBD. The barrier height of the Ni/n-type Ge SBDs with Ta-oxide interlayer was higher than the conventional Ni/n-type Ge SBD, implying that Ta-oxide interlayer led to the modification of the effective barrier height by influencing the space-region of n-type Ge. Moreover, when increasing thickness of Ta-oxide interlayer,

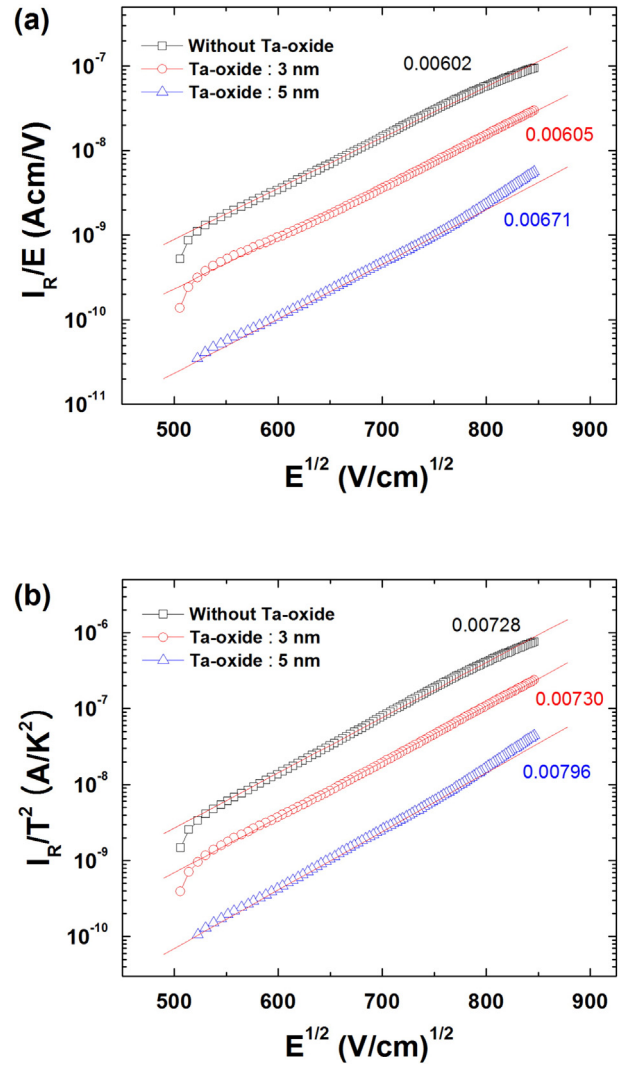


Fig. 6. Electric field dependence of the reverse leakage current in Ni/n-type Ge Schottky diodes with and without Ta-oxide interlayer; (a)  $I_R/E$  versus  $E^{1/2}$  plot for Poole-Frenkel emission mechanism, and (b)  $I_R/T^2$  versus  $E^{1/2}$  plot for Schottky emission mechanism.

barrier height increased and ideality factor decreased. XPS Ta 4f spectral results revealed that  $\text{Ta}^{4+}/\text{Ta}^{5+}$  ratio of 5 nm-thick interlayer was much lower than that of 3 nm-thick interlayer, indicating the presence of more stoichiometric Ta-oxide ( $\text{Ta}_2\text{O}_5$ ) having less defects in Ni/n-type Ge SBDs with 5 nm-thick Ta-oxide interlayer. Namely, due to the improvement of interface quality of Schottky junction caused by thicker Ta-oxide interlayer, Ni/n-type Ge SBDs with 5 nm-thick Ta-oxide interlayer exhibited lower interface states and ideality factor, as compared to Ni/n-type Ge SBDs with 3 nm-thick Ta-oxide interlayer. From the electric field dependence of the reverse current, the primary process involved in the leakage current of Ni/n-type Ge SBDs with and without Ta-oxide interlayer could be associated with Poole-Frenkel emission.

#### Acknowledgements

This research was supported by the Future Semiconductor Device Technology Development Program (Grant No. 10044651) funded by Ministry of Trade, Industry & Energy, Republic of Korea. It was also supported by Basic Science Research Program (NRF-2015R1A6A1A04020421) through the National Research Foundation of Korea (NRF) funded by the Ministry of Education, Republic of Korea.

## References

- [1] J. Oh, P. Majhi, H. Lee, O. Yoo, S. Banerjee, C.Y. Kang, J.W. Yang, R. Harris, H.H. Tseng, R. Jammy, Improved electrical characteristics of Ge-on-Si field-effect Transistors with controlled Ge epitaxial layer thickness on Si substrates, *IEEE Electron Dev. Lett.* 28 (2007) 1044–1046.
- [2] M.E. Aydin, N. Yildirim, A. Turut, Temperature-dependent behavior of Ni/4H-nSiC Schottky contacts, *J. Appl. Phys.* 102 (2007) 043701-1–043701-7.
- [3] A. Gumus, A. Turut, N. Yalcin, Temperature dependent barrier characteristics of CrNiCo alloy Schottky contacts on n-type molecular-beam epitaxy GaAs, *J. Appl. Phys.* 91 (2002) 245–250.
- [4] M.K. Hudait, S.B. Krupanidhi, Effects of thin oxide in metal–semiconductor and metal–insulator–semiconductor epi–GaAs Schottky diodes, *Solid State Electron.* 44 (2000) 1089–1097.
- [5] T. Sawada, Y. Ito, K. Imai, K. Suzuki, H. Tomozawa, S. Sakai, Electrical properties of metal/GaN and SiO<sub>2</sub>/GaN interfaces and effects of thermal annealing, *Appl. Surf. Sci.* 159–160 (2000) 449–455.
- [6] T. Hashizume, E. Alekseev, D. Pavlidis, K.S. Boutros, J. Redwing, Capacitance–voltage characterization of AlN/GaN metal–insulator–semiconductor structures grown on sapphire substrate by metalorganic chemical vapor deposition, *J. Appl. Phys.* 88 (2000) 1983–1986.
- [7] E. Arslan, Y. Safak, S. Altindal, O. Kelekci, E. Ozbay, Temperature dependent negative capacitance behavior in (Ni/Au)/AlGaIn/GaN heterostructures, *J. Non-Cryst. Solids* 356 (2010) 1006–1011.
- [8] A. Shetty, B. Roul, S. Mukundan, L. Mohan, G. Chandan, K.J. Vinoy, S.B. Krupanidhi, Temperature dependent electrical characterisation of Pt/HfO<sub>2</sub>/n–GaIn metal–insulator–semiconductor (MIS) Schottky diodes, *AIP Adv.* 5 (2015) 097103-1–097103-11.
- [9] S.M. Sze, *Physics of Semiconductor Devices*, second ed. John Wiley and Sons, New York, 1981.
- [10] E.H. Rhoderick, R.H. Williams, *Metal-Semiconductor Contacts*, second ed. Clarendon press, Oxford, 1988.
- [11] A. Dimoulas, P. Tsipas, A. Sotiropoulos, Fermi-level pinning and charge neutrality level in germanium, *Appl. Phys. Lett.* 89 (2006) 252110-1–252110-3.
- [12] T. Nishimura, K. Kita, A. Toriumi, Evidence for strong Fermi-level pinning due to metal-induced gap states at metal/germanium interface, *Appl. Phys. Lett.* 91 (2007) 123123-1–123123-3.
- [13] J.Y.J. Lin, A.M. Roy, A. Nainani, Y. Sun, K.C. Saraswat, Increase in current density for metal contacts to n-germanium by inserting TiO<sub>2</sub> interfacial layer to reduce Schottky barrier height, *Appl. Phys. Lett.* 98 (2011) 092113-1–092113-3.
- [14] A. Chawanda, C. Nyamhere, F.D. Aurret, W. Mtangi, M. Diale, J.M. Nel, Thermal annealing behavior of platinum, nickel and titanium Schottky barrier diodes on n-Ge (100), *J. Alloys Compd.* 492 (2010) 649–655.
- [15] X.V. Li, M.K. Husain, M. Kiziroglou, C.H. de Groot, Inhomogeneous Ni/Ge Schottky barriers due to variation in Fermi-level pinning, *Microelectron. Eng.* 86 (2009) 1599–1602.
- [16] D.T. Quan, H. Hbib, High barrier height Au/n-type InP Schottky contacts with a PO<sub>x</sub>N<sub>y</sub>H<sub>z</sub> interfacial layer, *Solid State Electron.* 36 (1993) 339–344.
- [17] O. Gullu, S. Aydogan, A. Turut, High barrier Schottky diode with organic interlayer, *Solid State Commun.* 152 (2012) 381–385.
- [18] W. Monch, Barrier heights of real Schottky contacts explained by metal-induced gap states and lateral inhomogeneities, *J. Vac. Sci. Technol. B* 17 (1999) 1867–1876.
- [19] R.T. Tung, Electron transport at metal-semiconductor interfaces: General theory, *Phys. Rev. B* 45 (1992) 13509–13523.
- [20] S.K. Cheung, N.W. Cheung, Extraction of Schottky diode parameters from forward current–voltage characteristics, *Appl. Phys. Lett.* 49 (1986) 85–87.
- [21] H. Norde, A modified forward *I*–*V* plot for Schottky diodes with high series resistance, *J. Appl. Phys.* 50 (1979) 5052–5053.
- [22] I. Jyothi, V. Janardhanam, V.R. Reddy, C.J. Choi, Modified electrical characteristics of Pt/n-type Ge Schottky diode with a pyronine-B interlayer, *SuperlatticesMicrostruct.* 75 (2014) 806–817.
- [23] A.A. Kumar, V.R. Reddy, V. Janardhanam, H.D. Yang, H.J. Yun, C.J. Choi, Electrical properties of Pt/n-type Ge Schottky contact with PEDOT:PSS interlayer, *J. Alloys Compd.* 549 (2013) 18–21.
- [24] H.C. Card, E.H. Rhoderick, Studies of tunnel MOS diodes I. Interface effects in silicon Schottky diodes, *J. Phys. D: Appl. Phys.* 4 (1971) 1589–1601.
- [25] B.C. Bayer, M. Fouquet, R. Blume, C.T. Wirth, R.S. Weatherup, K. Ogata, A.K. Gericke, R. Schlogl, S. Hofmann, J. Robertson, Co-Catalytic solid-state reduction applied to carbon nanotube growth, *J. Phys. Chem. C* 116 (2012) 1107–1113.
- [26] A.P. Huang, P.K. Chu, Crystallization improvement of Ta<sub>2</sub>O<sub>5</sub> thin films by the addition of water vapor, *J. Cryst. Growth* 274 (2005) 73–77.
- [27] S. Uthanna, S.V.J. Chandra, P.S. Reddy, G.M. Rao, Effect of post-deposition annealing on the structural and electrical properties of dc magnetron sputtered Ta<sub>2</sub>O<sub>5</sub> films, *J. Phys. Conf. Ser.* 114 (2008) 012035-1–012035-6.
- [28] J.M. Kopfer, S.K. Colberg, D. Borchert, Capacitance–voltage characterization of silicon oxide and silicon nitride coatings as passivation layers for crystalline silicon solar cells and investigation of their stability against x-radiation, *Thin Solid Films* 519 (2011) 6525–6529.
- [29] E. Dubois, J.L. Bubendorff, Kinetics of scanned probe oxidation: Space-charge limited growth, *J. Appl. Phys.* 87 (2000) 8148–8154.
- [30] H. Wong, N. Zhan, K.L. Ng, M.C. Poon, C.W. Kok, Interface and oxide traps in high-k hafnium oxide films, *Thin Solid Films* 462–463 (2004) 96–100.
- [31] V. Janardhanam, H.K. Lee, K.H. Shim, H.B. Hong, S.H. Lee, K.S. Ahn, C.J. Choi, Temperature dependency and carrier transport mechanisms of Ti/p-type InP Schottky rectifiers, *J. Alloys Compd.* 504 (2010) 146–150.